

**Analyzing Type IIn Supernovae spectra to determine if  
some arise from runaway luminous blue variable stars**

**A THESIS  
SUBMITTED TO THE FACULTY OF THE GRADUATE SCHOOL  
OF THE UNIVERSITY OF MINNESOTA  
BY**

**Michael Makmur**

**IN PARTIAL FULFILLMENT OF THE REQUIREMENTS  
FOR THE DEGREE OF  
MASTER OF SCIENCE**

**Patrick L. Kelly**

**May, 2020**

© Michael Makmur 2020  
ALL RIGHTS RESERVED

# Acknowledgements

tbd

The data presented herein were obtained at the W. M. Keck Observatory, which is operated as a scientific partnership among the California Institute of Technology, the University of California and the National Aeronautics and Space Administration. The Observatory was made possible by the generous financial support of the W. M. Keck Foundation.

The author wishes to recognize and acknowledge the very significant cultural role and reverence that the summit of Maunakea has always had within the indigenous Hawaiian community. We are most fortunate to have the opportunity to use observations from this mountain.

This research has made use of the Keck Observatory Archive (KOA), which is operated by the W. M. Keck Observatory and the NASA Exoplanet Science Institute (NExScI), under contract with the National Aeronautics and Space Administration.

# Dedication

tbd

## **Abstract**

# Contents

<b>Acknowledgements</b>	<b>i</b>
<b>Dedication</b>	<b>ii</b>
<b>Abstract</b>	<b>iii</b>
<b>List of Tables</b>	<b>vi</b>
<b>List of Figures</b>	<b>vii</b>
<b>1 Introduction</b>	<b>1</b>
1.1 Supernovae . . . . .	1
1.1.1 Type IIn Supernovae . . . . .	1
1.2 Runaway Stars . . . . .	5
1.3 This thesis . . . . .	8
<b>2 Observations</b>	<b>9</b>
2.1 Observed SNe IIn . . . . .	9
2.2 DEIMOS . . . . .	9
2.3 H $\alpha$ $\lambda 6562$ . . . . .	10
<b>3 Analysis</b>	<b>13</b>
3.1 Reducing DEIMOS Images . . . . .	13
3.2 Analyzing Velocities of SNe IIn . . . . .	14
<b>4 Discussion</b>	<b>16</b>

<b>5 Conclusion</b>	<b>17</b>
<b>Appendix A. Glossary and Acronyms</b>	<b>21</b>
A.1 Glossary . . . . .	21
A.2 Acronyms . . . . .	21
<b>Appendix B. Images and Spectra</b>	<b>22</b>

# List of Tables

2.1	Table of observations . . . . .	10
3.1	List of SNe IIn and their offset velocities from their host galaxies . . . . .	15
A.1	Acronyms . . . . .	21

# List of Figures

1.1	Cartoon of the basic structure for a SN IIn	2
1.2	Plot comparing mass-loss rate and wind velocities of SN IIn to possible progenitors	4
1.3	Plot depicting how far a runaway star will travel before exploding in a SN	7
2.1	Image of SN 2015bf from DEIMOS	11
2.2	H $\alpha$ emission from SN 2013dz and its host galaxy	12
B.1	SN 2005R H $\alpha$ relative to host galaxy	22
B.2	SN 2007K H $\alpha$ relative to host galaxy	23
B.3	SN 2008en H $\alpha$ relative to host galaxy	23
B.4	SN 2008gm H $\alpha$ relative to host galaxy	24
B.5	SN 2010jl H $\alpha$ relative to host galaxy	24
B.6	SN 2012ab H $\alpha$ relative to host galaxy	25
B.7	SN 2013dz H $\alpha$ relative to host galaxy	25
B.8	SN 2013W H $\alpha$ relative to host galaxy	26
B.9	SN 2015bf H $\alpha$ relative to host galaxy	26

# Chapter 1

## Introduction

### 1.1 Supernovae

*Insert introduction to SNe. Talk about types of SN (I, II-P, subclasses) traditional view of stellar evolution towards SNe.*

#### 1.1.1 Type IIn Supernovae

Type IIn supernovae (SNe IIn) are a subclass of core collapse supernovae (CCSNe) which show strong, narrow Balmer lines of hydrogen in their spectra (Schlegel, 1990), making up approximately 10% of all CCSNe. It is expected that these narrow lines arise from the supernova shock interacting with a dense, pre-existing circumstellar medium (CSM) surrounding the progenitor star (Smith, 2017), though the exact origins of the CSM is still up for debate. No matter the progenitor, some sort of extreme mass-loss is required in the decades prior to the explosion in order to generate such a CSM.

Because of the dense, surrounding CSM, the basic structure of a SNe IIn differs significantly from other SNe. As seen in Fig. 1.1, Smith (2017) splits the SN IIn into four physical zones: the unshocked CSM (1), the shocked CSM (2), the shocked SN ejecta (3), and the freely expanding SN ejecta (4). At the boundaries of each zone are the forward and reverse shocks, as well as the cold dense shell (CDS) between zones 2 and 3. In a non-SNe IIn, an observer would see radiation emerging almost entirely from zone 4, but since the CSM is so dense for these explosions, each zone can provide significant contributions towards emitted radiation (Smith, 2017). As the explosion

progresses and the photosphere recedes into zones 2 and 3, the gas piled into the CDS is constantly reheated by the shock and emits strong H $\alpha$  intermediate-width lines.

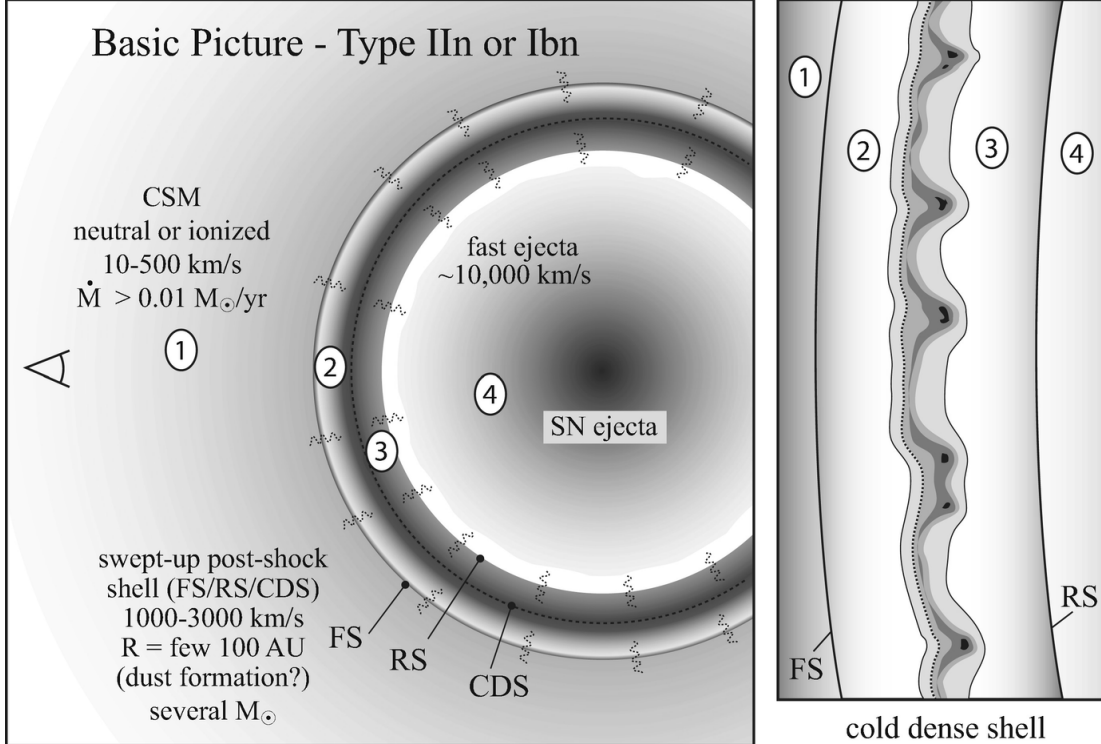


Figure 1.1: Cartoon of the basic structure of a SNe IIn. SNe IIn can be split into four separate zones: (1) the unshocked CSM, (2) the shocked CSM, (3) the shocked SN ejecta, and (4) freely expanding SN ejecta. At each boundary is a different event: between (1) and (2) exists the forward shock, between (2) and (3) is the cold dense shell (CDS), and between (3) and (4) is the reverse shock. X-rays and UV radiation can also be generated by the shock and propagate forwards into the CSM or back into the SN ejecta, and this is represented by the squiggly lines. This figure has been adapted from Smith et al. (2008).

It is important to remember that SNe IIn are an *external* phenomenon - they may actually mask other types of supernovae. Any type of core collapse supernova or even thermonuclear supernova can create the narrow Balmer lines seen in SNe IIn, so long as there is a dense enough hydrogen-rich medium surrounding the explosion (Smith, 2017). Because of this, it is impossible to trace SNe IIn to a single type of progenitor star or explosion type, and it may even be possible that SNe IIn are hiding novel explosion

types never observed before.

The luminosity of an SN IIn can be used to obtain information about the mass-loss rate of the progenitor star (Smith, 2017), allowing observers to determine other properties of the progenitor. SNe IIn can end up being much more luminous than other SNe, as the radiative shock from CSM interaction is extremely efficient at transforming the kinetic energy of the SN shockwave into visible-wavelength light (Smith, 2017). Because the luminosity is directly tied to the CSM, it can be expressed as

$$L = \frac{1}{2}wV_{\text{CDS}}^3 \quad (1.1)$$

where  $w$  represents the wind density parameter,  $w = \dot{M}/V_{\text{CSM}}$ , and  $V_{\text{CDS}}$  is the speed of the cold dense shell, the contact discontinuity where the SN shock and CSM meet (Smith, 2017).  $V_{\text{CDS}}$  can be estimated from the full width half maximum (FWHM) of intermediate-width lines in the optical spectrum, while  $V_{\text{CSM}}$ , the velocity of the CSM untouched by the SN shock, can be measured from narrower components. Combining this together, the mass-loss rate of the progenitor can be estimated by

$$\dot{M}_{\text{CSM}} = 2L \frac{V_{\text{CSM}}}{V_{\text{CDS}}^3} \quad (1.2)$$

One major caveat to this equation is that it requires a constant mass-loss rate and  $V_{\text{CSM}}$  over time in order to have the CSM density decrease as  $r^{-2}$ . If 1.2 is used when the CSM density profile is shallower, it will return a much larger mass-loss rate than is true (Dwarkadas, 2011). A review by Dwarkadas (2011) of several SNe IIn show that their mass-loss rates were overestimated, adding further confusion as to what the progenitors to these explosions are. Additionally, many SNe IIn show signs of significant asymmetries in their CSM, which will further alter the discrepancies between the results from the equation and the actual star.

Even with this setback, conclusions can be made about what kind of stars are able to produce fast enough winds and high enough mass-loss rates seen in SNe IIn. A plot from Smith (2017) comparing mass-loss rate and wind velocities of several SNe IIn and comparing them to progenitor properties can be seen in Fig. 1.2. It is worth noting that most SNe IIn require some sort of giant luminous blue variable (LBV) eruption in the decades preceding explosion to create enough CSM to form the narrow lines present in SNe IIn.

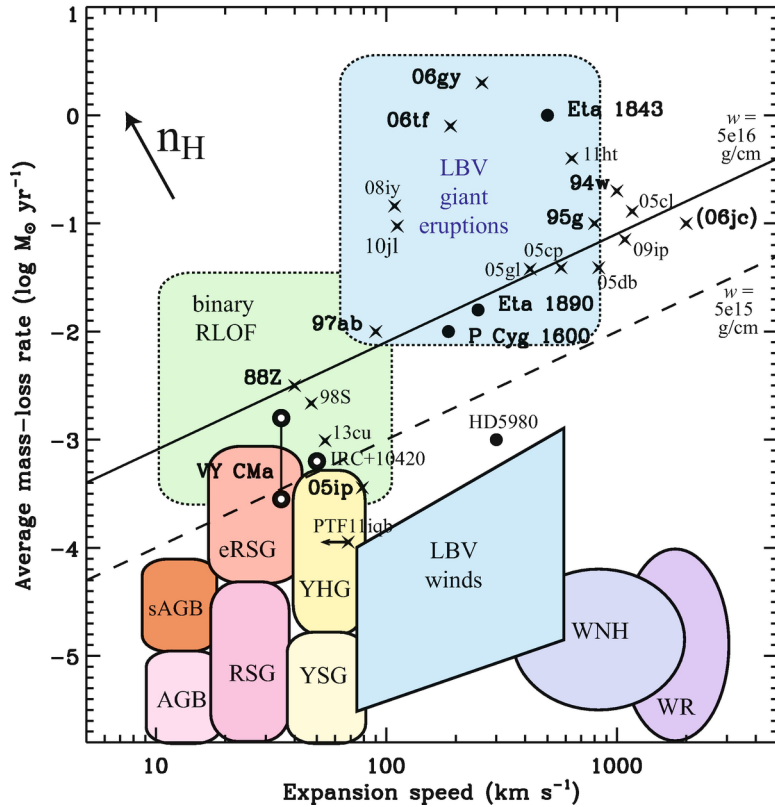


Figure 1.2: Plot of mass-loss rate as a function of wind velocity, with comparisons to known SNe IIn explosions and possible progenitor stars. Observational estimates of different SNe IIn are represented by X's, and some stars with high mass-loss (e.g.  $\eta$  Car) are represented by circles. The patches represent the approximate parameter spaces for different types of stars. Represented in this plot are asymptotic giant branch (AGB) and super-AGB (sAGB) stars, red supergiant (RSG) and extreme-RSGs, yellow super- and hypergiants (YSG, YHG), winds and eruptions from luminous blue variables (LBVs), Wolf Rayet stars (WR, WNH), as well as progenitors arising from basic binary Roche lobe overflow (RLOF). This figure was adapted from Smith (2017).

***Brief brief introduction to LBVs goes here?***

Referring back to Fig. 1.2, we see that while some IIn could arise from binary Roche lobe overflow (RLOF) or extreme red supergiants (eRSGs), it is clear that mass-loss estimates and wind speeds favor an LBV progenitor for most SNe IIn. Indeed, direct observations of progenitors for SNe IIn explosions such as SN 2009ip (Mauerhan et al., 2012, still debated) and SN 2010jl (Smith et al., 2011) appear to show a progenitor LBV in the location of the future explosion, though follow up observations to see if they are just SN imposters in the form of LBV eruptions are not common.

In terms of traditional stellar evolution models, however, having an LBV directly cause a SNe IIn is strongly opposed. These models treat LBVs as a short transition stage for an O-star, with its high mass-loss serving as an important stepping stone for the star to become an H-poor Wolf-Rayet (WR) star (Smith and Owocki, 2006). As mentioned before, Dwarkadas (2011) attempts to circumvent the necessity of a LBV by claiming that a clumpy CSM or an extremely short WR phase can also create the CSM necessary for SNe IIn, but the general consensus remains with LBVs as the main progenitor.

## 1.2 Runaway Stars

One hypothesis presented by Smith and Tombleson (2015) claims that approaching LBVs as runaway stars ejected from a binary system will allow them to become direct progenitors to SNe IIn.

Runaway stars are defined to have space velocities of 30 to 40 km s<sup>-1</sup> (Blaauw, 1961; Eldridge et al., 2011), though some can reach velocities over 200 km s<sup>-1</sup>. As described in Eldridge et al. (2011), the two main scenarios to create runaway stars are through a dynamical ejection scenario (DES) and through a binary supernova scenario (BSS), though the fastest runaway stars could have been created by a combination of both. In the DES, stars would be ejected via encounters with other massive stars in a dense cluster - this can be single stars or even entire binary systems of stars. The BSS, on the other hand, involves when one of the stars in a binary explodes, unbinding the system and kicking the secondary star. The two methods are expected to contribute roughly equal amounts of runaway stars, but it is possible to differentiate between the

two by looking at their compositions as BSS runaways should show evidence of binary interaction (Eldridge et al., 2011). Again, since entire binary systems can be ejected in DES, it is reasonable to assume that some of those binary systems undergo BSS as well.

The most common type of runaway star are O- and B-type stars (Blaauw, 1961), massive stars that can lead to core collapse explosions. Since these stars are launched in excess of  $30 \text{ km s}^{-1}$ , it is not unreasonable that secondary stars kicked in a BSS could travel many parsecs before exploding in their own SN. The simulations run by Eldridge et al. (2011) (seen in Fig. 1.3) do in fact find that for Type II SNe as well as Type Ib and Ic SNe that these progenitors can be launched in excess of 100 pc from the star-forming region they were born in.

While Eldridge et al. (2011) does not look at SNe IIn specifically, Habergham et al. (2014) analyzes 39 SNe IIn and SN imposters and looking to see how it follows H $\alpha$  emission (a tracer of star formation) in their host galaxies. Based on these observations, Habergham et al. (2014) conclude that not only do SNe IIn not correlate to star formation regions, they correlate even less to star formation than other explosions such as SNe II-P. The authors attribute this as an indication that SNe IIn are unlikely to have high mass progenitors, as they expect them to follow star forming regions as well as SN Ic, which have massive progenitors as well. This implies that whatever progenitor is creating Type IIn explosions must either be low enough mass to survive longer than higher mass stars, or they have been isolated by some other means.

Although this appears to be contradictory, observations of LBVs in the Milky Way (MW), Large Magellanic Cloud (LMC), and Small Magallanic Cloud (SMC) imply that LBV stars almost always find themselves isolated from other O-type stars and star-forming regions (Smith and Tombleson, 2015). This matches up nicely with the generally accepted view of LBVs serving as the progenitors for SNe IIn.

In order to reconcile the fact that LBVs according to stellar evolution models should not be found isolated, Smith and Tombleson (2015) suggest that most LBV stars are actually the end stage for the kicked mass gaining companion in the BSS. With the LBV progenitor being kicked from its binary, it can then travel the adequate distance to be found later in a region of relative isolation from other O-type stars and star forming regions. The important aspect of this scenario is that the LBV progenitor, serving as the secondary star, accretes mass through RLOF from the primary star prior to the

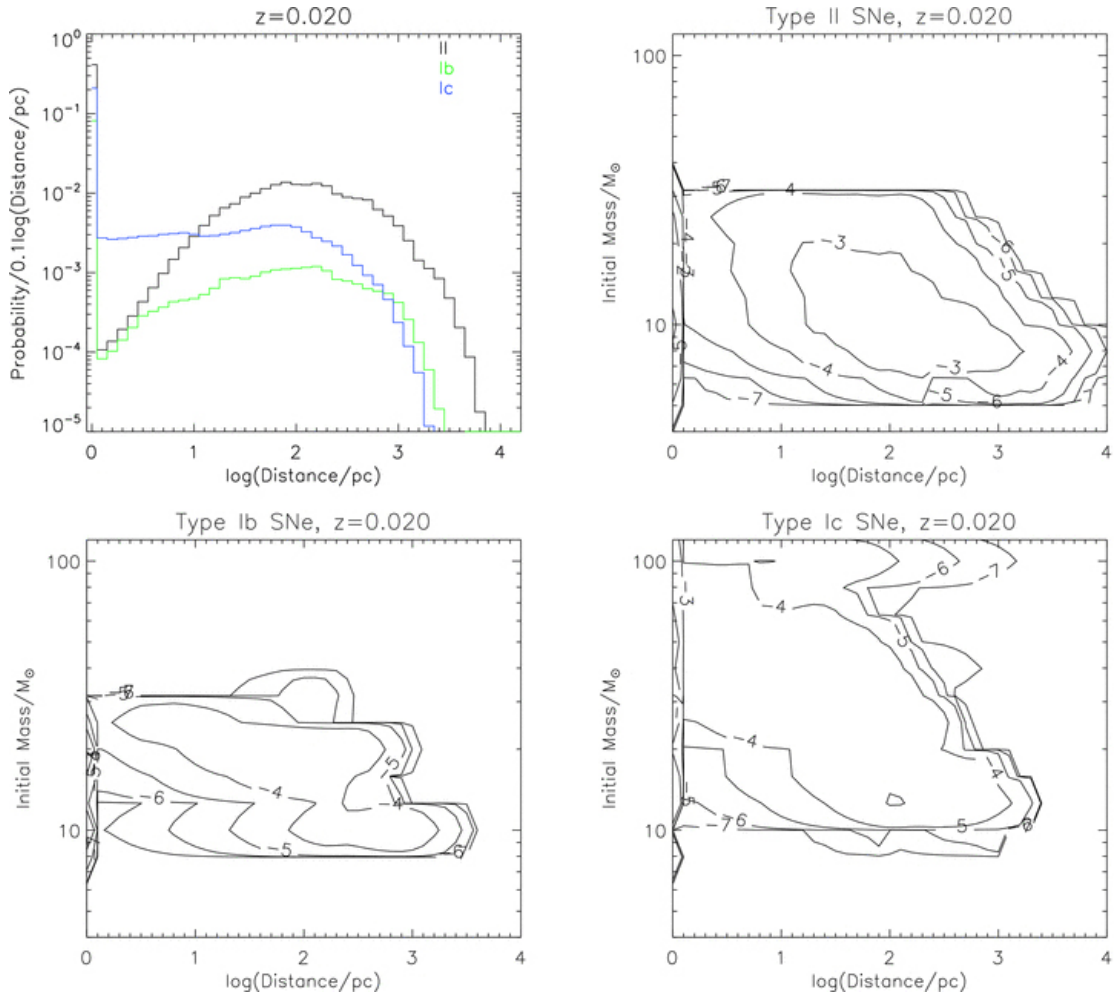


Figure 1.3: Plot showing the distribution of distance traveled by SN progenitors versus the progenitor's original mass, in solar metallicity. The data comes from the simulations of Eldridge et al. (2011). The contours represent the probability in  $\log_{10}$  of a SN progenitor of that initial mass traveling that distance. This figure has been adapted from Eldridge et al. (2011).

primary star's explosion. This allows the star to substantially increase its own mass and luminosity, and therefore appear younger than the stars around it (these are known as "blue stragglers") (Smith and Tombleson, 2015). These stars will still have an extended lifetime compared to stars of their new mass and luminosity, and as such can travel great distances before evolving and exploding (Smith and Tombleson, 2015). Additionally, the process of RLOF will allow them to gain significant angular momentum and velocity, which may be important to LBV instabilities and eruptions (Smith and Tombleson, 2015).

### 1.3 This thesis

The goal of this thesis is to determine if we see evidence of SNe IIn arising from runaway stars, and if so, place constraints on them in the hope of learning more about their progenitors. In order to do this, I will be analyzing the narrow H $\alpha$  lines of SNe IIn and comparing their line of sight velocities to the expected radial velocity of the galaxy in that location.

Chapter 2 will detail the observed supernovae I use in this thesis, as well as how they were obtained. Chapter 3 will talk about the methods used to analyze the offset velocities of the SNe IIn relative to their host galaxies. Chapter 4 will detail the findings of this thesis as well as any future work that can be done from here. Finally, Chapter 5 will conclude the findings of this thesis.

# Chapter 2

## Observations

### 2.1 Observed SNe IIn

All observations used for this thesis were taken with the DEIMOS (DEep Imaging Multi-Object Spectrograph) multi-object spectrograph on the Keck II (10-m) telescope (Faber et al., 2003). In order to collect as many SNe IIn as possible, a list of SNe IIn was obtained using the Asiago Supernova Catalog (Barbon et al., 1999), a catalog of supernovae dating from 1885 to 2017, as well as the Transient Name Server<sup>1</sup> from the International Astronomical Union. These were then searched in the Keck Observatory Archive to see if any observations were taken of the SNe with DEIMOS. Upon analysis, we also removed any SNe IIn that had already evolved to the point where the SN ejecta was freely expanding (there were no more narrow- or intermediate-width H $\alpha$  lines). All observations used in this thesis are listed in Table 2.1. *Of note: many more SN were downloaded than were analyzed due to errors with the DEIMOS pipeline.*

### 2.2 DEIMOS

DEIMOS is a multi-object spectrograph capable of taking spectra of multiple objects at once. The slitmasks span 16.7' of the sky, and have a wavelength range of 4100 Å to 1.1  $\mu$ m (Faber et al., 2003). The observations used in this thesis all utilize the Long Variable Multislit (LVM) slitmask. All observations taken prior to 2008 utilized four

---

<sup>1</sup> <https://wis-tns.weizmann.ac.il/>

SN	Date (UT)	Galaxy Host	Grating Used	PI
SN 2015bf	2016 Jan 7	NGC 7653	600ZD	Filippenko, A.
SN 2013dz	2013 Aug 2	Unknown	1200G	Filippenko, A.
SN 2013W	2013 Apr 8	UGC 5448	600ZD	Filippenko, A.
SN 2012ab	2012 Nov 15	Unknown	600ZD	Filippenko, A.
SN 2008gm	2012 Sep 23	NGC 7530	1200G	Filippenko, A.
SN 2008en	2012 Sep 23	UGC 564	1200G	Filippenko, A.
SN 2010jl	2010 Nov 7	UGC 5189A	600ZD	Filippenko, A.
SN 2007K	2007 Jan 22	MCG +06-20-50	600ZD	Tonry, J.
SN 2005R	2005 Feb 11	UGC 6274	600ZD	Davis, M.

Table 2.1: Table of observations

slitlets on the original LVM, while future ones use the LVMslitB or LVMslitC which have 5 slitlets.

DEIMOS has two separate gratings: a lower-resolution aluminized grating with 600 lines mm<sup>-1</sup> (600ZD) blazed at 7500 Å which offers a width of 5300 Å; and a higher-resolution gold-coated grating with 1200 lines mm<sup>-1</sup> (1200G) blazed at 7500 Å offering a width of 2630 Å.

Fig. 2.1 shows an image of SN 2015bf prior to being reduced in the DEIMOS pipeline. This image is transposed and rotated such that the *x* axis represents wavelength (increasing to the right) and the *y* axis represents the location of the emission. Several night-sky emission lines from the atmosphere can be seen in this image, and are removed in the pipeline.

### 2.3 H $\alpha$ λ6562

H $\alpha$  is the primary Balmer line of hydrogen, occurring when a hydrogen electron moves from the third energy level to the second energy level. As mentioned in Chapter 1, we expect to see strong emissions of H $\alpha$  in spectra of SNe IIn due to the shock heating of the CDS. We additionally would expect to see H $\alpha$  tracing the SN host galaxy, as it traces high mass stars and star formation rates (as mentioned in Habergham et al. (2014)).

Since DEIMOS is a multi-object spectrograph, we can expect to see the SN continuum, the SN H $\alpha$ , and the host galaxy H $\alpha$  in the same image. An example of this can

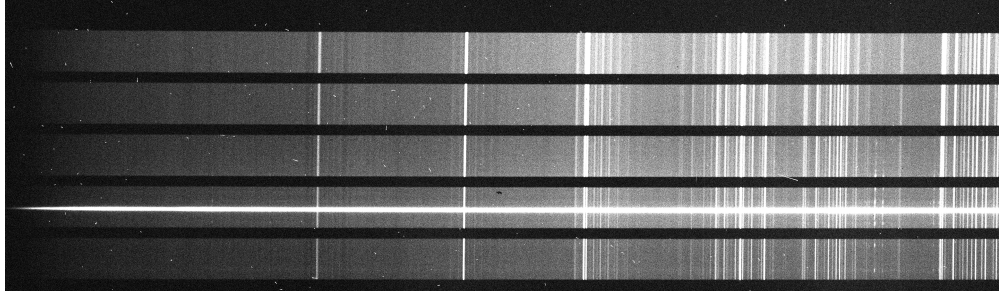


Figure 2.1: An image taken of the blue portion SN 2015bf on DEIMOS, prior to being reduced. This image has transposed and rotated such that the  $x$  axis represents wavelength (increasing to the right) and the  $y$  axis represents location in the CCD. The SN continuum is clearly visible in the second slit from the left, though there are many skylines still present. This image was taken as part of the Keck-UC Time-domain Exploration.

be seen in Fig. 2.2, which displays the  $\text{H}\alpha$  of SN 2013dz and its host galaxy. What is typically seen in these observations is a bright continuum emission from the SN, making it difficult to visually distinguish the  $\text{H}\alpha$  emission. We also see a fainter (though it is not depicted as such in Fig. 2.2)  $\text{H}\alpha$  emission that traces the host galaxy's emission.

One property of this image that is easy to notice is that the galactic  $\text{H}\alpha$  shifts from left to right in wavelength. This is expected, as this shift represents the Doppler shift of different parts of the galaxy. In Fig. 2.2, the bottom portion of the galaxy is blueshifted, indicating its line of sight velocity is pointed towards the observer, while the top portion is redshifted. This shift can be used to estimate what radial velocity is expected of the SN IIIn if it were not a runaway star.

#### *Example $\text{H}\alpha$ spectrum?*

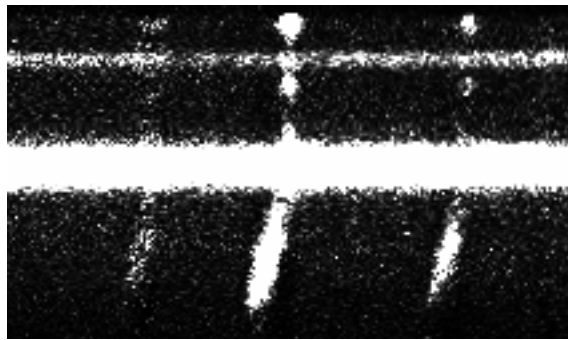


Figure 2.2: An image taken of the red portion of SN 2013dz on DEIMOS, after being reduced. We can clearly see the H $\alpha$  emission from the host galaxy as well as the continuum emission of SN 2013dz. We also can see N II  $\lambda$ 6548 and N II  $\lambda$ 6583 lines of the host galaxy. The H $\alpha$  emission of the SN is difficult to distinguish visually as the SN continuum is already extremely bright.

# Chapter 3

## Analysis

### 3.1 Reducing DEIMOS Images

We used the Carnegie Python Distribution (CarPy)<sup>1</sup> in order to handle, calibrate, reduce, and analyze the images observed from DEIMOS (Kelson et al., 1999; Kelson, 2003). CarPy includes many routines for processing multi-slit spectroscopic data. The CarPy environment also contains PyRAF, a Python based command language to run IRAF (Image Reduction and Analysis Facility) tasks. PyRAF is a product of the Space Telescope Science Institute, which is operated by AURA for NASA.

Our reduction is based on the standard prescription outlined in Silverman et al. (2012), with slight modifications. Since all of the observations were made on the same instrument (DEIMOS), the only changes that need to be made between different observations is based on the placement of the slitlets, the number of slitlets, and the resolution of the gratings. I will summarize the our pipeline below:

1. Subtract out the overscan region and subtract out the bias. For this, we use `iraf.ccdproc`. Then transpose the image and rotate it 180 degrees such that wavelength is increasing in the  $+x$  direction of the image.
2. Combine and normalize the flat-fields using `iraf.flatcombine`.
3. Rectify the image using the combined flat-fields. The  $y$ -distortion is calculated using `getrect` and then applied to the flats using `copyrect` such that the wavelength

---

<sup>1</sup> <https://code.obs.carnegiescience.edu/carnegie-python-distribution>

in every vertical strip is the same.

4. Find the locations of the slitlets in the images using `findslits`. Once the slits are found, the locations are written to the image header and copied to the rest of the images.
5. Divide out the flat fields and the blaze from the other images using `flat2d`.
6. Get the rectification for each slit using `getrect`, and then copy them to all the other images using `copyrect`. In this step, we are specifically copying the  $x$ -distortion.
7. Calibrate the wavelength scale with `wavrect`. This uses the assistance of arc-lamp spectra, which typically contained Neon, Argon, Krypton, and Xenon, and sometimes Cadmium, Zinc, and Mercury. This gets applied to all the images.
8. Extract the 1D spectra of the standard star using `iraf.apall`. We interactively remove telluric and absorption features using `iraf.splot` to select the regions and then dividing them out using `iraf.sarith`. This forms a standard continuum spectrum, as well as a sensitivity function.
9. Extract the 1D spectra of the SN, and normalize by the standard continuum. Apply telluric corrections using `iraf.telluric`, and flux calibrate using the sensitivity function.
10. Combine the spectra of the blue and red sides to form one complete spectrum. We can then analyze the location of the peak as well as get a full-width half-maximum measurement of the H $\alpha$  using `splot`.

### 3.2 Analyzing Velocities of SNe IIn

- Obtain central location of H $\alpha$  for multiple points in the galaxy as well as the SN
- Plot all these points and fit a polynomial fit through them
- Utilize line of sight velocity  $v = \frac{c\Delta\lambda}{\lambda}$  to determine the relative velocity of the SN compared to the galaxy at that location

- Find results for the 9 SN in Table 3.1

SN	Velocity (km s <sup>-1</sup> )
SN 2015bf	51.42
SN 2013dz	39.31
SN 2013W	18.49
SN 2012ab	13.27
SN 2008gm	7.49
SN 2008en	1.98
SN 2010jl	37.46
SN 2007K	115.12
SN 2005R	23.3

Table 3.1: List of SNe IIn and their offset velocities from their host galaxies

## Chapter 4

# Discussion

- Most lower than 30, some higher than 30 - how does this fit with the paradigm from Smith and Tombleson (2015)? projection effects, external phenomenon, etc play a factor. Also wow the one that's over 100 km/s - it has PCygni so should be CDS
- Small sample size! Very difficult to reach a good conclusion
- Implications of runaways being progenitors - yes? maybe? eh
- Implications on LBVs as the progenitors - nothing here says it's not possible
- See if you can find any literature on these SN. I'm pretty sure we have 2010jl

## **Chapter 5**

# **Conclusion**

Meh. Maybe???

# References

- R. Barbon, V. Buondí, E. Cappellaro, and M. Turatto. The Asiago Supernova Catalogue - 10 years after. *Astronomy and Astrophysics Supplement Series*, 139(3):531–536, 11 1999. ISSN 03650138. doi: 10.1051/aas:1999404.
- A. Blaauw. On the origin of the O and B-type stars with high velocities. *Bulletin of the Astronomical Institutes of the Netherlands*, 15:265, 1961. ISSN 0004-6361.
- V. Dwarkadas. On luminous blue variables as the progenitors of core-collapse supernovae, especially Type IIn supernovae. *Monthly Notices of the Royal Astronomical Society*, 412(3):1639–1649, 4 2011. ISSN 00358711. doi: 10.1111/j.1365-2966.2010.18001.x.
- John J. Eldridge, Norbert Langer, and Christopher A. Tout. Runaway stars as progenitors of supernovae and gamma-ray bursts. *Monthly Notices of the Royal Astronomical Society*, 414(4):3501–3520, 3 2011. ISSN 00358711. doi: 10.1111/j.1365-2966.2011.18650.x.
- Sandra M. Faber, Andrew C. Phillips, Robert I. Kibrick, Barry Alcott, Steven L. Allen, Jim Burrous, T. Cantrall, De Clarke, Alison L. Coil, David J. Cowley, Marc Davis, William T. S. Deich, Ken Dietsch, David K. Gilmore, Carol A. Harper, David F. Hilyard, Jeffrey P. Lewis, Molly McVeigh, Jeffrey Newman, Jack Osborne, Ricardo Schiavon, Richard J. Stover, Dean Tucker, Vernon Wallace, Mingzhi Wei, Gregory Wirth, and Christopher A. Wright. The DEIMOS spectrograph for the Keck II Telescope: integration and testing. In Masanori Iye and Alan F. M. Moorwood, editors, *Instrument Design and Performance for Optical/Infrared Ground-based Telescopes*, volume 4841, page 1657. SPIE, 3 2003. doi: 10.1117/12.460346.

- S. M. Habergham, J. P. Anderson, P. A. James, and J. D. Lyman. Environments of interacting transients: Impostors and Type IIn supernovae. *Monthly Notices of the Royal Astronomical Society*, 441(3):2230–2252, 4 2014. ISSN 13652966. doi: 10.1093/mnras/stu684.
- Daniel D. Kelson, Garth D. Illingworth, Pieter G. van Dokkum, and Marijn Franx. The Evolution of Early-Type Galaxies in Distant Clusters II: Internal Kinematics of 55 Galaxies in the  $z=0.33$  Cluster CL1358+62. *The Astrophysical Journal*, 531(1):159–183, 8 1999. doi: 10.1086/308445. URL <http://arxiv.org/abs/astro-ph/9908257><http://dx.doi.org/10.1086/308445>.
- Daniel D. Kelson. Optimal Techniques in Two-dimensional Spectroscopy: Background Subtraction for the 21st Century. *Publications of the Astronomical Society of the Pacific*, 115(808):688–699, 6 2003. ISSN 0004-6280. doi: 10.1086/375502.
- Jon C. Mauerhan, Nathan Smith, Alexei Filippenko, Kyle Blanchard, Peter Blanchard, Chadwick F. E. Casper, S. Bradley Cenko, Kelsey I. Clubb, Daniel Cohen, Kiera Fuller, Gary Li, and Jeffrey M. Silverman. The Unprecedented 2012 Outburst of SN 2009ip: A Luminous Blue Variable Becomes a True Supernova. 9 2012. doi: 10.1093/mnras/stt009. URL <http://arxiv.org/abs/1209.6320><http://dx.doi.org/10.1093/mnras/stt009><http://arxiv.org/abs/1209.6320%0A><http://dx.doi.org/10.1093/mnras/stt009>.
- E. Schlegel. A new subclass of type II supernovae? *Monthly Notices of the Royal Astronomical Society*, 244(2):269–271, 1990. ISSN 0035-8711.
- Jeffrey M. Silverman, Ryan J. Foley, Alexei V. Filippenko, Mohan Ganeshalingam, Aaron J. Barth, Ryan Chornock, Christopher V. Griffith, Jason J. Kong, Nicholas Lee, Douglas C. Leonard, Thomas Matheson, Emily G. Miller, Thea N. Steele, Brian J. Barris, Joshua S. Bloom, Bethany E. Cobb, Alison L. Coil, Louis Benoit Desroches, Elinor L. Gates, Luis C. Ho, Saurabh W. Jha, Michael T. Kandrashoff, Weidong Li, Kaisey S. Mandel, Maryam Modjaz, Matthew R. Moore, Robin E. Mostardi, Marina S. Papenkova, Sung Park, Daniel A. Perley, Dovi Poznanski, Cassie A. Reuter, James Scala, Franklin J.D. Serduke, Joseph C. Shields, Brandon J. Swift, John L. Tonry, Schuyler D. Van Dyk, Xiaofeng Wang, and S. Diane. Berkeley Supernova

- Ia Program - I. Observations, data reduction and spectroscopic sample of 582 low-redshift Type Ia supernovae. *Monthly Notices of the Royal Astronomical Society*, 425(3):1789–1818, 9 2012. ISSN 00358711. doi: 10.1111/j.1365-2966.2012.21270.x.
- Nathan Smith. Interacting Supernovae: Types IIn and Ibn. In *Handbook of Supernovae*, pages 403–429. Springer International Publishing, 12 2017. doi: 10.1007/978-3-319-21846-5\\_\\_38.
- Nathan Smith and Stanley P. Owocki. On the Role of Continuum-driven Eruptions in the Evolution of Very Massive Stars and Population III Stars. *The Astrophysical Journal*, 645(1):L45–L48, 7 2006. ISSN 0004-637X. doi: 10.1086/506523.
- Nathan Smith and Ryan Tombleson. Luminous blue variables are antisocial: Their isolation implies that they are kicked mass gainers in binary evolution. *Monthly Notices of the Royal Astronomical Society*, 447(1):598–617, 6 2015. ISSN 13652966. doi: 10.1093/mnras/stu2430.
- Nathan Smith, Ryan Chornock, Weidong Li, Mohan Ganeshalingam, Jeffrey M. Silverman, Ryan J. Foley, Alexei V. Filippenko, and Aaron J. Barth. SN 2006tf: Precursor Eruptions and the Optically Thick Regime of Extremely Luminous Type IIn Supernovae. *The Astrophysical Journal*, 686(1):467–484, 10 2008. ISSN 0004-637X. doi: 10.1086/591021.
- Nathan Smith, Weidong Li, Adam A. Miller, Jeffrey M. Silverman, Alexei V. Filippenko, Jean Charles Cuillandre, Michael C. Cooper, Thomas Matheson, and Schuyler D. Van Dyk. A massive progenitor of the luminous type IIn supernova 2010jl. *Astrophysical Journal*, 732(2), 11 2011. ISSN 15384357. doi: 10.1088/0004-637X/732/2/63.

# Appendix A

## Glossary and Acronyms

Care has been taken in this thesis to minimize the use of jargon and acronyms, but this cannot always be achieved. This appendix defines jargon terms in a glossary, and contains a table of acronyms and their meaning.

### A.1 Glossary

- **Object** – definition

### A.2 Acronyms

Table A.1: Acronyms

Acronym	Meaning
CSM	Circumstellar medium
SN	Supernova (plural supernovae, SNe)
SNe II $\mathrm{n}$	Supernovae Type II-narrow

## Appendix B

# Images and Spectra

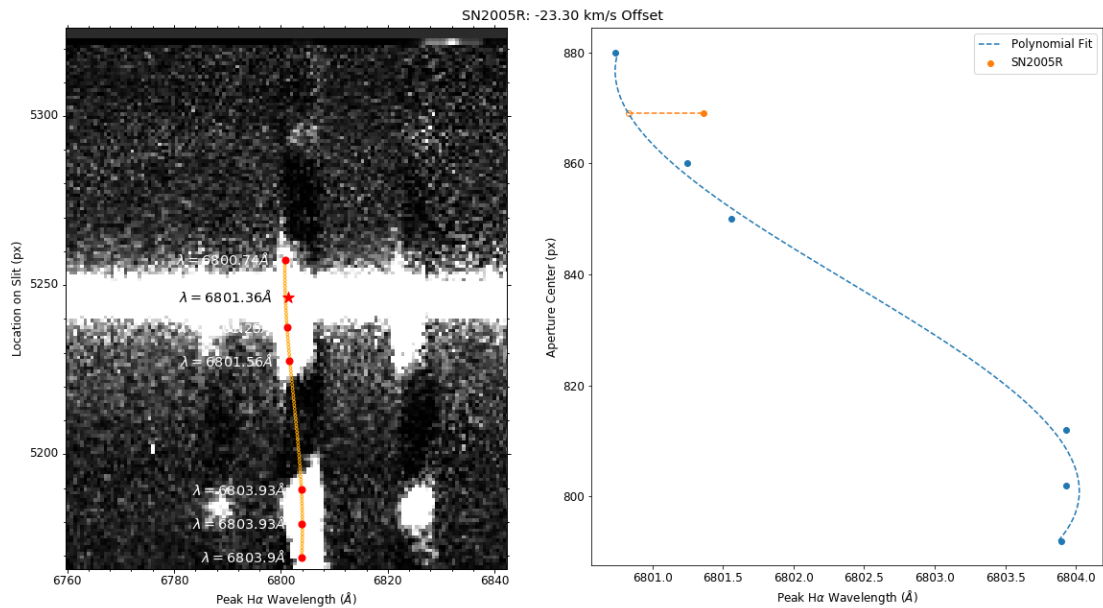
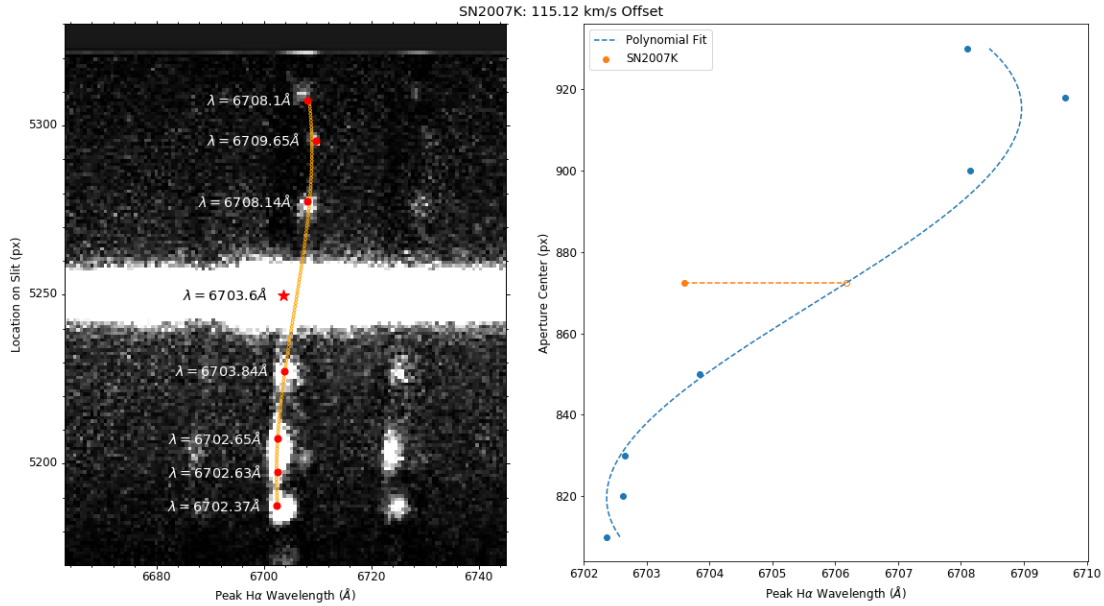
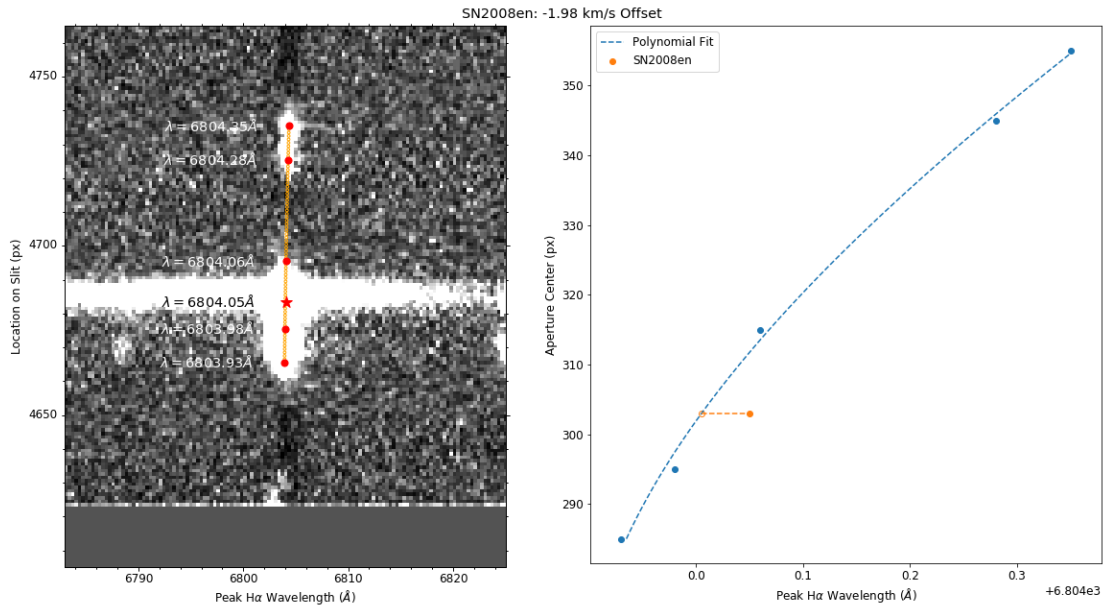
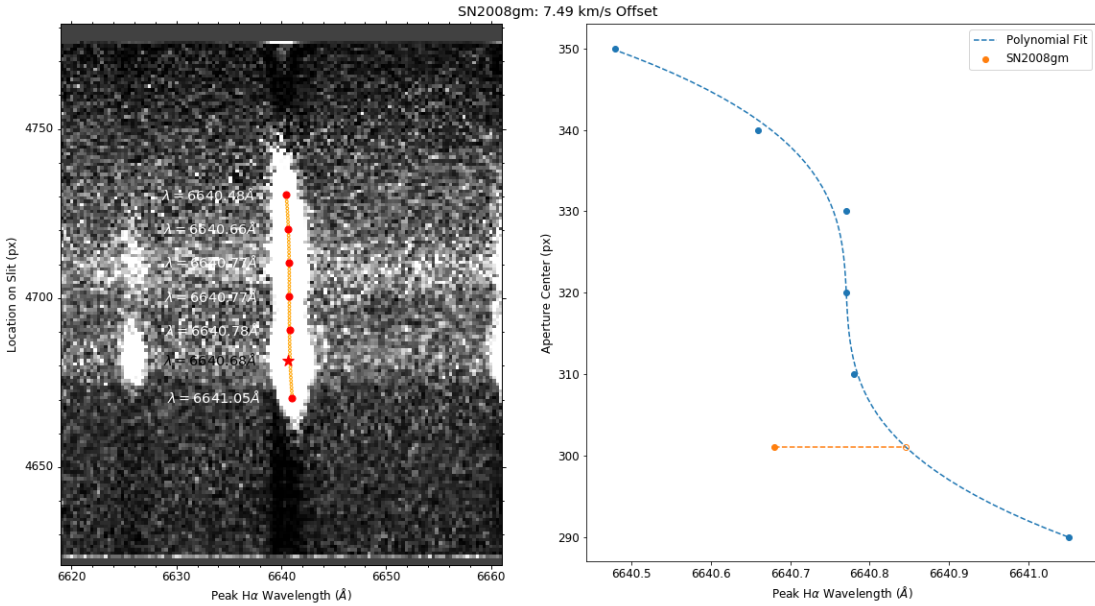
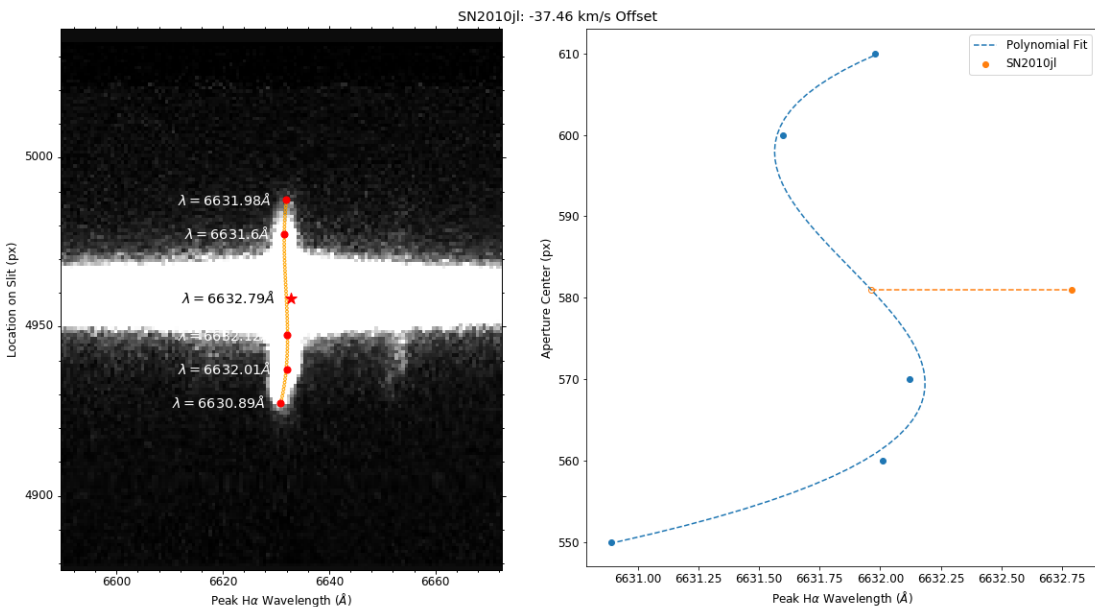
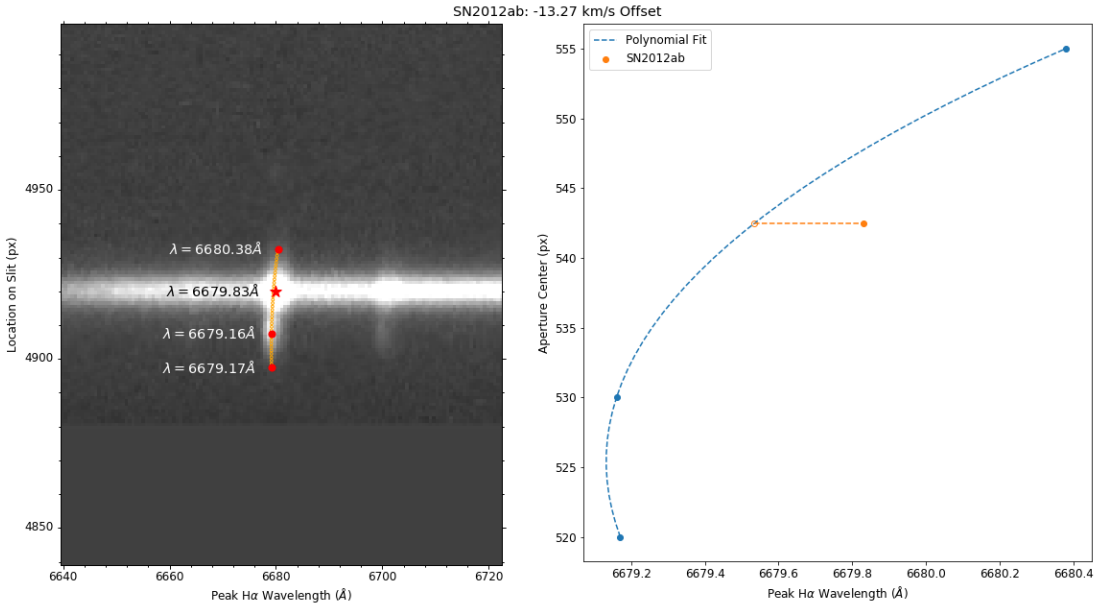
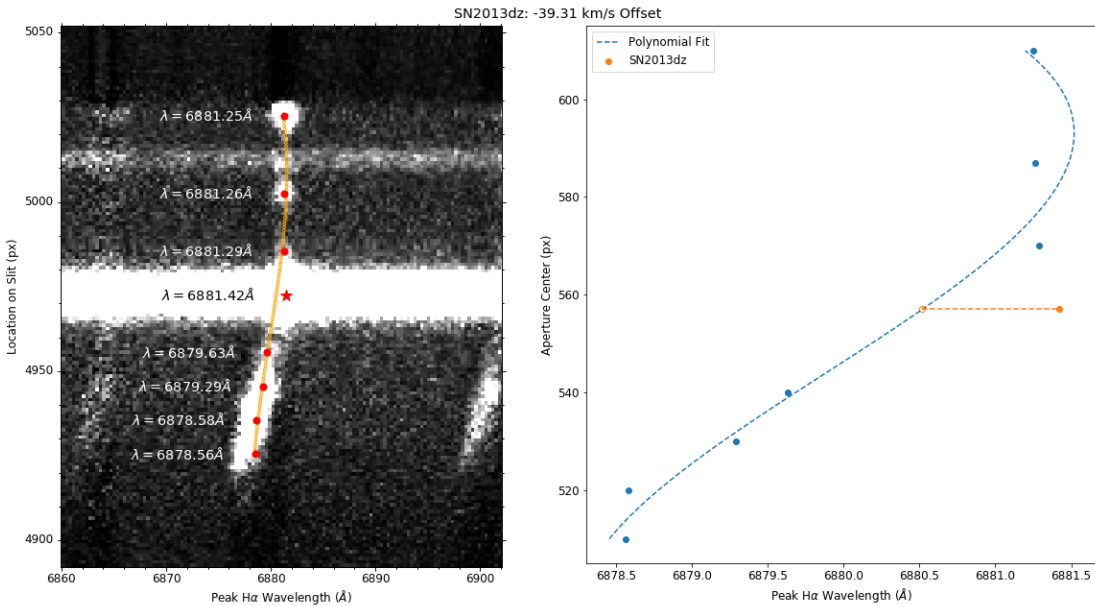
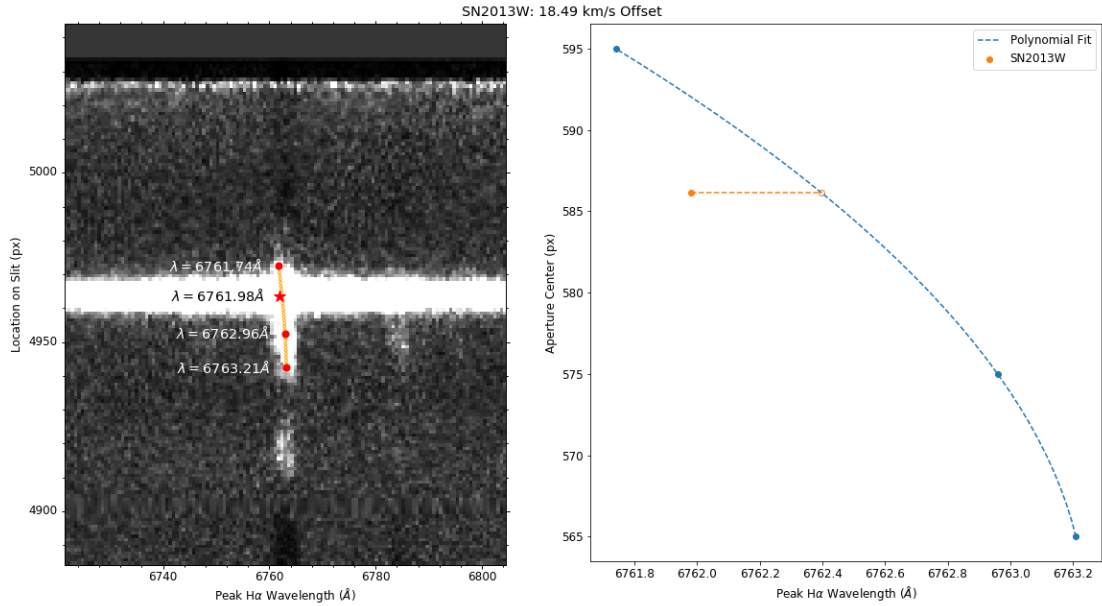
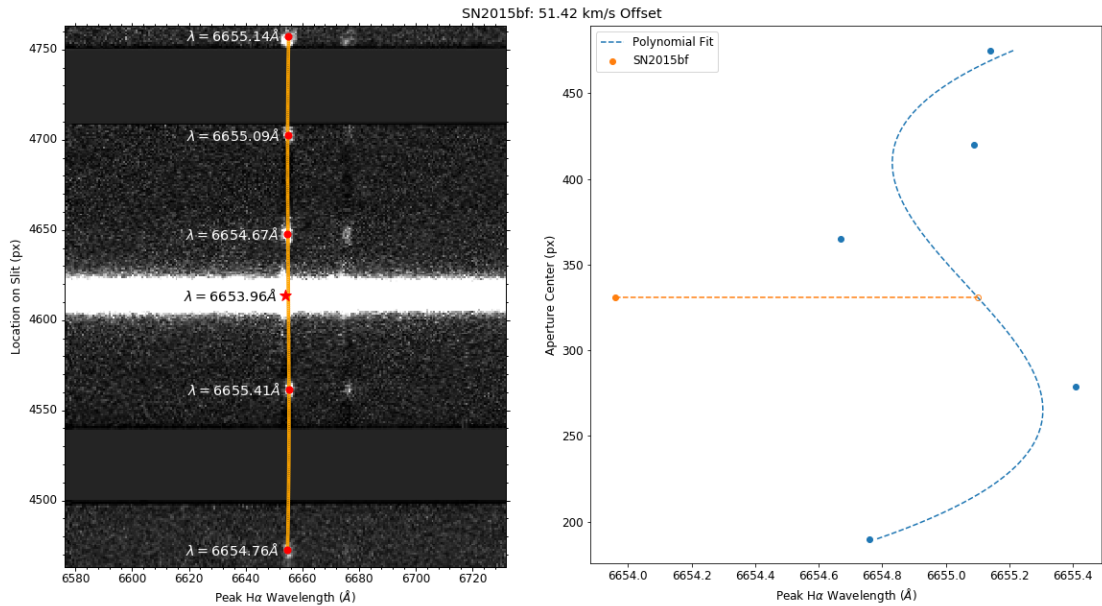


Figure B.1: SN 2005R H $\alpha$  relative to host galaxy

Figure B.2: SN 2007K H $\alpha$  relative to host galaxyFigure B.3: SN 2008en H $\alpha$  relative to host galaxy

Figure B.4: SN 2008gm H $\alpha$  relative to host galaxyFigure B.5: SN 2010jl H $\alpha$  relative to host galaxy

Figure B.6: SN 2012ab H $\alpha$  relative to host galaxyFigure B.7: SN 2013dz H $\alpha$  relative to host galaxy

Figure B.8: SN 2013W H $\alpha$  relative to host galaxyFigure B.9: SN 2015bf H $\alpha$  relative to host galaxy